

Singapore Management University

Institutional Knowledge at Singapore Management University

Research Collection School Of Computing and Information Systems

School of Computing and Information Systems

6-1995

The forward-backward asymmetry for charm quarks at the Z pole

D. BUSKULIC

Manoj THULASIDAS

Singapore Management University, manojt@smu.edu.sg

Follow this and additional works at: https://ink.library.smu.edu.sg/sis_research



Part of the [Databases and Information Systems Commons](#), and the [Programming Languages and Compilers Commons](#)

Citation

1

This Journal Article is brought to you for free and open access by the School of Computing and Information Systems at Institutional Knowledge at Singapore Management University. It has been accepted for inclusion in Research Collection School Of Computing and Information Systems by an authorized administrator of Institutional Knowledge at Singapore Management University. For more information, please email cherylds@smu.edu.sg.

The Forward-Backward Asymmetry for Charm Quarks at the Z

The ALEPH Collaboration¹

Abstract

The data set collected with the ALEPH detector from 1991 to 1995 at LEP has been analysed to measure the charm forward-backward asymmetry at the Z. Out of a total of 4.1 million hadronic Z decays, about 36000 high momentum D^{*+} , D^+ and D^0 decays were reconstructed, of which 80% originate from $Z \rightarrow c\bar{c}$ events. The forward-backward asymmetry was measured at three energy points:

$$\begin{aligned} A_{FB}^c(\sqrt{s} = 89.37 \text{ GeV}) &= (-1.0 \pm 4.4)\% \\ A_{FB}^c(\sqrt{s} = 91.22 \text{ GeV}) &= (6.3 \pm 1.0)\% \\ A_{FB}^c(\sqrt{s} = 92.96 \text{ GeV}) &= (11.0 \pm 3.4)\% . \end{aligned}$$

From this analysis, a value of the effective electroweak mixing angle $\sin^2 \theta_W^{\text{eff}} = 0.2321 \pm 0.0016$ is extracted.

(To be submitted to Physics Letters B)

¹See next pages for the list of authors

The ALEPH Collaboration

R. Barate, D. Buskulic, D. Decamp, P. Ghez, C. Goy, J.-P. Lees, A. Lucotte, E. Merle, M.-N. Minard, J.-Y. Nief, B. Pietrzyk

Laboratoire de Physique des Particules (LAPP), IN²P³-CNRS, F-74019 Annecy-le-Vieux Cedex, France

R. Alemany, G. Boix, M.P. Casado, M. Chmeissani, J.M. Crespo, M. Delfino, E. Fernandez, M. Fernandez-Bosman, Ll. Garrido,¹⁵ E. Graugès, A. Juste, M. Martinez, G. Merino, R. Miquel, Ll.M. Mir, I.C. Park, A. Pascual, I. Riu, F. Sanchez

Institut de Física d'Altes Energies, Universitat Autònoma de Barcelona, E-08193 Bellaterra (Barcelona), Spain⁷

A. Colaleo, D. Creanza, M. de Palma, G. Gelao, G. Iaselli, G. Maggi, M. Maggi, S. Nuzzo, A. Ranieri, G. Raso, F. Ruggieri, G. Selvaggi, L. Silvestris, P. Tempesta, A. Tricomi,³ G. Zito

Dipartimento di Fisica, INFN Sezione di Bari, I-70126 Bari, Italy

X. Huang, J. Lin, Q. Ouyang, T. Wang, Y. Xie, R. Xu, S. Xue, J. Zhang, L. Zhang, W. Zhao

Institute of High-Energy Physics, Academia Sinica, Beijing, The People's Republic of China⁸

D. Abbaneo, U. Becker, P. Bright-Thomas,²⁴ D. Casper, M. Cattaneo, F. Cerutti, V. Ciulli, G. Dissertori, H. Drevermann, R.W. Forty, M. Frank, R. Hagelberg, A.W. Halley, J.B. Hansen, J. Harvey, P. Janot, B. Jost, I. Lehraus, P. Mato, A. Minten, L. Moneta,²¹ A. Pacheco, F. Ranjard, L. Rolandi, D. Rousseau, D. Schlatter, M. Schmitt,²⁰ O. Schneider, W. Tejessy, F. Teubert, I.R. Tomalin, H. Wachsmuth

European Laboratory for Particle Physics (CERN), CH-1211 Geneva 23, Switzerland

Z. Ajaltouni, F. Badaud, G. Chazelle, O. Deschamps, A. Falvard, C. Ferdi, P. Gay, C. Guicheney, P. Henrard, J. Jousset, B. Michel, S. Monteil, J-C. Montret, D. Pallin, P. Perret, F. Podlyski, J. Proriot, P. Rosnet

Laboratoire de Physique Corpusculaire, Université Blaise Pascal, IN²P³-CNRS, Clermont-Ferrand, F-63177 Aubière, France

J.D. Hansen, J.R. Hansen, P.H. Hansen, B.S. Nilsson, B. Rensch, A. Wäänänen

Niels Bohr Institute, DK-2100 Copenhagen, Denmark⁹

G. Daskalakis, A. Kyriakis, C. Markou, E. Simopoulou, I. Siotis, A. Vayaki

Nuclear Research Center Demokritos (NRCD), GR-15310 Attiki, Greece

A. Blondel, G. Bonneaud, J.-C. Brient, P. Bourdon, A. Rougé, M. Rumpf, A. Valassi,⁶ M. Verderi, H. Videau

Laboratoire de Physique Nucléaire et des Hautes Energies, Ecole Polytechnique, IN²P³-CNRS, F-91128 Palaiseau Cedex, France

E. Focardi, G. Parrini, K. Zachariadou

Dipartimento di Fisica, Università di Firenze, INFN Sezione di Firenze, I-50125 Firenze, Italy

M. Corden, C. Georgiopoulos, D.E. Jaffe

Supercomputer Computations Research Institute, Florida State University, Tallahassee, FL 32306-4052, USA^{13,14}

A. Antonelli, G. Bencivenni, G. Bologna,⁴ F. Bossi, P. Campana, G. Capon, V. Chiarella, G. Felici, P. Laurelli, G. Mannocchi,⁵ F. Murtas, G.P. Murtas, L. Passalacqua, M. Pepe-Altarelli

Laboratori Nazionali dell'INFN (LNF-INFN), I-00044 Frascati, Italy

L. Curtis, J.G. Lynch, P. Negus, V. O'Shea, C. Raine, J.M. Scarr, K. Smith, P. Teixeira-Dias, A.S. Thompson, E. Thomson

Department of Physics and Astronomy, University of Glasgow, Glasgow G12 8QQ, United Kingdom¹⁰

O. Buchmüller, S. Dhamotharan, C. Geweniger, G. Graefe, P. Hanke, G. Hansper, V. Hepp, E.E. Kluge, A. Putzer, J. Sommer, K. Tittel, S. Werner, M. Wunsch

*Institut für Hochenergiephysik, Universität Heidelberg, D-69120 Heidelberg, Germany*¹⁶

R. Beuselinck, D.M. Binnie, W. Cameron, P.J. Dornan,² M. Girone, S. Goodsir, E.B. Martin, N. Marinelli, A. Moutoussi, J. Nash, J.K. Sedgbeer, P. Spagnolo, M.D. Williams

*Department of Physics, Imperial College, London SW7 2BZ, United Kingdom*¹⁰

V.M. Ghete, P. Girtler, E. Kneringer, D. Kuhn, G. Rudolph

*Institut für Experimentalphysik, Universität Innsbruck, A-6020 Innsbruck, Austria*¹⁸

A.P. Betteridge, C.K. Bowdery, P.G. Buck, P. Colrain, G. Crawford, A.J. Finch, F. Foster, G. Hughes, R.W.L. Jones, N.A. Robertson, M.I. Williams

*Department of Physics, University of Lancaster, Lancaster LA1 4YB, United Kingdom*¹⁰

I. Giehl, C. Hoffmann, K. Jakobs, K. Kleinknecht, G. Quast, B. Renk, E. Rohne, H.-G. Sander, P. van Gemmeren, C. Zeitnitz

*Institut für Physik, Universität Mainz, D-55099 Mainz, Germany*¹⁶

J.J. Aubert, C. Benchouk, A. Bonissent, G. Bujosa, J. Carr,² P. Coyle, F. Etienne, O. Leroy, F. Motsch, P. Payre, M. Talby, A. Sadouki, M. Thulasidas, K. Trabelsi

Centre de Physique des Particules, Faculté des Sciences de Luminy, IN²P³-CNRS, F-13288 Marseille, France

M. Aleppo, M. Antonelli, F. Ragusa

Dipartimento di Fisica, Università di Milano e INFN Sezione di Milano, I-20133 Milano, Italy

R. Berlich, V. Büscher, G. Cowan, H. Dietl, G. Ganis, G. Lütjens, C. Mannert, W. Männer, H.-G. Moser, S. Schael, R. Settles, H. Seywerd, H. Stenzel, W. Wiedenmann, G. Wolf

*Max-Planck-Institut für Physik, Werner-Heisenberg-Institut, D-80805 München, Germany*¹⁶

J. Boucrot, O. Callot, S. Chen, A. Cordier, M. Davier, L. Dufлот, J.-F. Grivaz, Ph. Heusse, A. Höcker, A. Jacholkowska, D.W. Kim,¹² F. Le Diberder, J. Lefrançois, A.-M. Lutz, M.-H. Schune, E. Tournefier, J.-J. Veillet, I. Videau, D. Zerwas

Laboratoire de l'Accélérateur Linéaire, Université de Paris-Sud, IN²P³-CNRS, F-91898 Orsay Cedex, France

P. Azzurri, G. Bagliesi,² G. Batignani, S. Bettarini, T. Boccali, C. Bozzi, G. Calderini, M. Carpinelli, M.A. Ciocci, R. Dell'Orso, R. Fantechi, I. Ferrante, L. Foà,¹ F. Forti, A. Giassi, M.A. Giorgi, A. Gregorio, F. Ligabue, A. Lusiani, P.S. Marrocchesi, A. Messineo, F. Palla, G. Rizzo, G. Sanguinetti, A. Sciabà, G. Sguazzoni, R. Tenchini, G. Tonelli,¹⁹ C. Vannini, A. Venturi, P.G. Verdini

Dipartimento di Fisica dell'Università, INFN Sezione di Pisa, e Scuola Normale Superiore, I-56010 Pisa, Italy

G.A. Blair, L.M. Bryant, J.T. Chambers, M.G. Green, T. Medcalf, P. Perrodo, J.A. Strong, J.H. von Wimmersperg-Toeller

*Department of Physics, Royal Holloway & Bedford New College, University of London, Surrey TW20 OEX, United Kingdom*¹⁰

D.R. Botterill, R.W. Clift, T.R. Edgecock, P.R. Norton, J.C. Thompson, A.E. Wright

*Particle Physics Dept., Rutherford Appleton Laboratory, Chilton, Didcot, Oxon OX11 0QX, United Kingdom*¹⁰

B. Bloch-Devaux, P. Colas, S. Emery, W. Kozanecki, E. Lançon,² M.-C. Lemaire, E. Locci, P. Perez, J. Rander, J.-F. Renardy, A. Roussarie, J.-P. Schuller, J. Schwindling, A. Trabelsi, B. Vallage

*CEA, DAPNIA/Service de Physique des Particules, CE-Saclay, F-91191 Gif-sur-Yvette Cedex, France*¹⁷

S.N. Black, J.H. Dann, R.P. Johnson, H.Y. Kim, N. Konstantinidis, A.M. Litke, M.A. McNeil, G. Taylor

*Institute for Particle Physics, University of California at Santa Cruz, Santa Cruz, CA 95064, USA*²²

C.N. Booth, S. Cartwright, F. Combley, M.S. Kelly, M. Lehto, L.F. Thompson

*Department of Physics, University of Sheffield, Sheffield S3 7RH, United Kingdom*¹⁰

K. Affholderbach, A. Böhrer, S. Brandt, C. Grupen, P. Saraiva, L. Smolik, F. Stephan

*Fachbereich Physik, Universität Siegen, D-57068 Siegen, Germany*¹⁶

G. Giannini, B. Gobbo, G. Musolino

Dipartimento di Fisica, Università di Trieste e INFN Sezione di Trieste, I-34127 Trieste, Italy

J. Rothberg, S. Wasserbaech

Experimental Elementary Particle Physics, University of Washington, WA 98195 Seattle, U.S.A.

S.R. Armstrong, E. Charles, P. Elmer, D.P.S. Ferguson, Y. Gao, S. González, T.C. Greening, O.J. Hayes, H. Hu, S. Jin, P.A. McNamara III, J.M. Nachtman,²³ J. Nielsen, W. Orejudos, Y.B. Pan, Y. Saadi, I.J. Scott, J. Walsh, Sau Lan Wu, X. Wu, G. Zobernig

*Department of Physics, University of Wisconsin, Madison, WI 53706, USA*¹¹

¹Now at CERN, 1211 Geneva 23, Switzerland.

²Also at CERN, 1211 Geneva 23, Switzerland.

³Also at Dipartimento di Fisica, INFN, Sezione di Catania, Catania, Italy.

⁴Also Istituto di Fisica Generale, Università di Torino, Torino, Italy.

⁵Also Istituto di Cosmo-Geofisica del C.N.R., Torino, Italy.

⁶Supported by the Commission of the European Communities, contract ERBCHBICT941234.

⁷Supported by CICYT, Spain.

⁸Supported by the National Science Foundation of China.

⁹Supported by the Danish Natural Science Research Council.

¹⁰Supported by the UK Particle Physics and Astronomy Research Council.

¹¹Supported by the US Department of Energy, grant DE-FG0295-ER40896.

¹²Permanent address: Kangnung National University, Kangnung, Korea.

¹³Supported by the US Department of Energy, contract DE-FG05-92ER40742.

¹⁴Supported by the US Department of Energy, contract DE-FC05-85ER250000.

¹⁵Permanent address: Universitat de Barcelona, 08208 Barcelona, Spain.

¹⁶Supported by the Bundesministerium für Bildung, Wissenschaft, Forschung und Technologie, Germany.

¹⁷Supported by the Direction des Sciences de la Matière, C.E.A.

¹⁸Supported by Fonds zur Förderung der wissenschaftlichen Forschung, Austria.

¹⁹Also at Istituto di Matematica e Fisica, Università di Sassari, Sassari, Italy.

²⁰Now at Harvard University, Cambridge, MA 02138, U.S.A.

²¹Now at University of Geneva, 1211 Geneva 4, Switzerland.

²²Supported by the US Department of Energy, grant DE-FG03-92ER40689.

²³Now at University of California at Los Angeles (UCLA), Los Angeles, CA 90024, U.S.A.

²⁴Now at School of Physics and Astronomy, Birmingham B15 2TT, U.K.

1 Introduction

The forward-backward asymmetry in $Z \rightarrow c\bar{c}$ decays provides a direct and precise test of the coupling of the Z to up-type quarks. The asymmetry A_{FB}^f in $Z \rightarrow f\bar{f}$ decays arises from parity violation in Z production and decay. In the Standard Model, the differential cross section, expressed as a function of the angle θ between the outgoing fermion and the incoming electron, is

$$\frac{1}{\sigma} \frac{d\sigma}{d\cos\theta} = \frac{3}{8}(1 + \cos^2\theta) + A_{FB}^f \cos\theta \quad (1)$$

At the Z pole, for unpolarised e^+e^- beams, A_{FB}^f is related to the pole asymmetry $A_{FB}^{0,f}$, defined in terms of the effective couplings in the improved Born approximation as

$$A_{FB}^{0,f} = \frac{3}{4} \frac{2g_{Ve}g_{Ae}}{(g_{Ve}^2 + g_{Ae}^2)} \frac{2g_{Vf}g_{Af}}{(g_{Vf}^2 + g_{Af}^2)}. \quad (2)$$

The measurement can be interpreted in terms of the effective electroweak mixing angle $\sin^2\theta_W^{\text{eff}} = \frac{1}{4}(1 - g_{Ve}/g_{Ae})$.

The $Z \rightarrow c\bar{c}$ decays provide a convenient way to directly test the Z coupling to up-type quarks, since the $Z \rightarrow u\bar{u}$ events are much harder to isolate. In this paper a sample of $Z \rightarrow c\bar{c}$ decays is selected using high energy D^+ , D^0 and D^{*+} , fully reconstructed from their decay products. The restricted number of usable decay channels limits the tagging efficiency. On the other hand, the high purity obtained in the selection, together with a minor dependence on the decay models, allow a measurement with small systematic uncertainties.

First the selection of charmed mesons is described, then the background estimate is discussed and the asymmetry is measured on the selected sample at three different centre of mass energies: at the Z peak and at ± 2 GeV off-peak.

2 Reconstruction of $D^{(*)}$ mesons

A detailed description of the ALEPH detector and its performance can be found in Ref. [1, 2]. Charged particles are detected in the central part of the detector, consisting of a two-layer silicon vertex detector with double-sided (r - ϕ and z) readout, a cylindrical drift chamber and a large time projection chamber (TPC), which together measure up to 33 coordinates along the charged particle trajectories. Tracking is performed in a 1.5 T axial magnetic field provided by a superconducting solenoid. The TPC also provides up to 338 measurements of ionization (dE/dx) allowing particle identification. The electromagnetic calorimeter is a lead/wire-chamber sandwich operated in proportional mode. It is read out in projective towers of typically 15×15 mrad² size segmented in three longitudinal sections. The iron return yoke is instrumented with streamer tubes to provide a measurement of the hadronic energy. An energy flow algorithm [2] combines charged particles momenta and calorimetric energy measurements and provides a list of energy flow particles on which the analysis is based.

About four million hadronic Z decays are selected as described in Ref. [3], out of the data set collected by ALEPH during the 1991–1995 running period at the Z resonance.

Table 1: *Results of the D^+ , D^0 and D^{*+} reconstruction. The second column shows the number of candidates in the different channels, while the last column shows the number of signal events, after combinatorial background subtraction, together with the statistical and systematic uncertainties.*

Decay channel	Candidates	Signal
$D^{*+} \rightarrow \pi_s^+ K^- \pi^+$	5022	$4434 \pm 71 \pm 55$
$D^{*+} \rightarrow \pi_s^+ K^- \pi^+ \pi^0$	7327	$5429 \pm 86 \pm 124$
$D^0 \rightarrow K^- \pi^+$	7682	$5032 \pm 97 \pm 75$
$D^{*+} \rightarrow \pi_s^+ K^- \pi^+ \pi^+ \pi^-$	14565	$8710 \pm 121 \pm 276$
$D^{*+} \rightarrow \pi_s^+ K^- \pi^+ (\pi^0)$	10766	$5824 \pm 104 \pm 322$
$D^+ \rightarrow K^- \pi^+ \pi^+$	12664	$6357 \pm 113 \pm 102$

Charmed mesons are reconstructed in the following decay modes (charge-conjugate modes are implied throughout the paper):

$$\begin{array}{ll}
 (i) & D^{*+} \rightarrow D^0 \pi_s^+ \\
 & \quad \quad \quad \hookrightarrow K^- \pi^+ \\
 (ii) & D^{*+} \rightarrow D^0 \pi_s^+ \\
 & \quad \quad \quad \hookrightarrow K^- \pi^+ \pi^0 \\
 (iii) & D^0 \rightarrow K^- \pi^+ \\
 (iv) & D^{*+} \rightarrow D^0 \pi_s^+ \\
 & \quad \quad \quad \hookrightarrow K^- \pi^+ \pi^+ \pi^- \\
 (v) & D^{*+} \rightarrow D^0 \pi_s^+ \\
 & \quad \quad \quad \hookrightarrow K^- \pi^+ + (\pi^0) \\
 (vi) & D^+ \rightarrow K^- \pi^+ \pi^+
 \end{array}$$

where the soft pion from D^{*+} decay is indicated as π_s^+ . Channel (v) is selected without reconstructing the π^0 by using the kinematic properties of the underlying resonances in the D^0 decay that make the $K^- \pi^+$ invariant mass peak near $1.6 \text{ GeV}/c^2$. The reconstruction proceeds from channel (i) to channel (vi); once a candidate has been found in one event, this event is excluded in the following channels. Consequently, the $D^0 \rightarrow K^- \pi^+$ decays from D^{*+} are removed from the inclusive sample (iii), thus avoiding double counting. The number of candidates for each selected sample is listed in Table 1.

All combinations of two and four tracks or two tracks and a π^0 , with total null charge, are considered as D^0 candidates, and all combinations of three tracks with total charge +1 are considered as D^+ candidates. The π^0 candidates are selected from two-photon combinations having a χ^2 probability of at least 5% for a mass-constrained kinematical fit [3]. The invariant mass of the D candidates, with mass assignment according to particle hypothesis, is required to be close to the D meson mass within two times the invariant mass resolution. The $D^0 \rightarrow K^- \pi^+ + (\pi^0)$ channel is reconstructed as the $D^0 \rightarrow K^- \pi^+$ decays, except that candidates are kept if the $K^- \pi^+$ invariant mass is between $1.5 \text{ GeV}/c^2$ and $1.7 \text{ GeV}/c^2$.

D^{*+} candidates from $D^{*+} \rightarrow \pi_s^+ D^0$ decays are selected by adding an extra track with momentum less than $3.5 \text{ GeV}/c$ to a D^0 candidate. In the channels (ii), (iv) and (v) the combinatorial background is reduced by requiring the D^0 candidate to satisfy $|\cos \theta^*| \leq 0.8$, where θ^* , in the D^0 rest frame, is the angle between the D^0 direction and the sphericity axis of the three ($D^0 \rightarrow K^- \pi^+ \pi^0$) or four ($D^0 \rightarrow K^- \pi^+ \pi^+ \pi^-$) decay products, or the kaon direction in the decay $D^0 \rightarrow K^- \pi^+ (\pi^0)$ with an undetected π^0 . The π_s^+ momentum is required to be greater than $1.5 \text{ GeV}/c$, favoring high momentum

D^{*+} 's, in order to reject combinatorial background and $Z \rightarrow b\bar{b}$ events in which a b hadron decays into a D^{*+} . In Figure 1 the mass difference $\Delta M = M_{D^{*+}} - M_{D^0}$ distributions are shown. Candidates are selected in the ΔM region $143.5 \text{ MeV}/c^2$ to $147.5 \text{ MeV}/c^2$ for the channels (i), (ii) and (iv) and $141 \text{ MeV}/c^2$ to $152 \text{ MeV}/c^2$ for channel (v).

Candidates from $D^0 \rightarrow K^-\pi^+$ decays, channel (iii), are selected if the kaon track momentum is greater than $2.5 \text{ GeV}/c$ and the pion track momentum greater than $1.5 \text{ GeV}/c$. A common vertex is searched for and candidates are kept if a vertex with a χ^2 probability greater than 1% is found, and the projected decay length significance is greater than unity. The asymmetry measurement in this channel suffers from the presence of a significant contribution of fake candidates due to incorrect mass assignments, which reverse the charge assignment of the charm quark. For a large fraction of these candidates, the correct mass assignment is also selected in the event. The dE/dx measurements of the two tracks are used to choose between the two mass combinations. The probability to be a kaon (P_K) or a pion (P_π) is computed from the measured track ionization and the expectation for a kaon or a pion. The mass assignment which gives the highest probability $P_K \times P_\pi$ is kept. If no dE/dx measurement is available for the tracks, the choice is made randomly. This criterion reduces the contribution from incorrect mass assignments to 4% in the signal region.

D^+ candidates, channel (vi), are selected if the kaon track has a momentum greater than $2.5 \text{ GeV}/c$ and if the dE/dx measurement is more consistent with the expectation for a kaon than for a pion. One of the two pion tracks is required to have a momentum greater than $1.5 \text{ GeV}/c$, the other pion momentum being greater than $0.75 \text{ GeV}/c$. The three tracks are required to form a common vertex with a χ^2 probability greater than 1%, and a significance of the decay length, projected along the D^+ momentum, greater than 1.5. Finally, in case of multiple candidates, only the candidate with the largest decay length significance is kept.

The contribution of the $Z \rightarrow c\bar{c}$ process to the $D^0 \rightarrow K^-\pi^+$ and $D^+ \rightarrow K^-\pi^+\pi^+$ signals is enhanced to 80% by selecting D^0 and D^+ candidates with energy greater than half the beam energy. The resulting invariant mass distributions are shown in Figure 2 for the $D^0 \rightarrow K^-\pi^+$ sample and in Figure 3 for the $D^+ \rightarrow K^-\pi^+\pi^+$ sample.

3 Combinatorial background estimate

The fraction of combinatorial background events in the D^{*+} sample is estimated from the mass difference distributions. The data sample contains, in addition to D^{*+} 's which are correctly reconstructed, a combinatorial background and a fraction of D^{*+} 's obtained from soft pions and partially reconstructed or fake D^0 's. The latter contribution, clearly seen in Figure 1(c), carries the correct charm quark charge, so it is treated as signal. The mass difference of the combinatorial background is obtained from D^0 candidates in Monte Carlo simulated events in which no D^{*+} 's have been produced. A track from fragmentation is added to such candidates and the combinatorial background is estimated from the resulting ΔM distribution, normalized to the data in the region $\Delta M > 0.16 \text{ GeV}/c^2$. In the background normalisation procedure reflections of the signal in the $\Delta M > 0.16 \text{ GeV}/c^2$ region have to be taken into account. This is done by using, both in data and in background Monte Carlo, only events in which a signal candidate is not found.

The fraction of combinatorial background events in the D^0 and D^+ samples is extracted from a fit to the invariant mass distributions (Figures 2 and 3). The D^0 and D^+ signals are parametrized by two Gaussians with a common mean and the combinatorial background by a polynomial function. Resonant background contributions, such as $D^0 \rightarrow K^-K^+, \pi^+\pi^-(\pi^0)$ and $D^0 \rightarrow K^-\pi^+$ where the two mass assignments are reversed (D^0 channel), $D_s^\pm \rightarrow \phi\pi^\pm$ and $D_s^\pm \rightarrow K^*K$ (D^+ channel), are taken into account in the fit. Their shapes and sizes are fixed by the Monte Carlo simulation with branching ratio according to PDG values [4].

The fitted numbers of signal events in the different channels are shown in Table 1.

4 Measurement of the forward-backward asymmetry

The measurement of the differential cross section for $Z \rightarrow c\bar{c}$ events (Eq. 1) requires the evaluation of the angle θ between the charm quark direction and the incident electron beam. This is measured from the thrust axis, oriented along the candidate direction, $\cos\theta = -Q \cos\theta_{\text{thrust}}$, Q being the electric charge of the reconstructed K in the D^0 or D^+ decays.

Together with charm events two possible sources contribute to the observed asymmetry: combinatorial background and charm mesons from $Z \rightarrow b\bar{b}$ events. Therefore the observed asymmetry in the selected sample is

$$A_{FB}^{\text{obs}} = f_{\text{sig}}f_c A_{FB}^c + f_{\text{sig}}(1 - f_c)A_{FB}^b + (1 - f_{\text{sig}})A_{FB}^{\text{bkg}}$$

where f_{sig} is the fraction of D mesons in the sample, f_c is the fraction originating from direct charm production and A_{FB}^{bkg} is the forward-backward asymmetry of the combinatorial background.

The fraction, f_c , of D mesons originating from direct charm production is measured directly from data [5]. The event is divided into two hemispheres according to the thrust axis. A lifetime-mass tag [6] is applied on the hemisphere opposite to the D meson, to select b hemispheres with 99% purity. The fraction, $f_{b\text{-tag}}$, of D mesons that survive the b -tag cut is used to extract the charm fraction $f_c = \frac{\epsilon_{b\bar{b}} - f_{b\text{-tag}}}{\epsilon_{b\bar{b}} - \epsilon_{c\bar{c}}}$, where $\epsilon_{b\bar{b}}$ and $\epsilon_{c\bar{c}}$ are the b -tag efficiency for b and charm events; $\epsilon_{c\bar{c}}$ is obtained from Monte Carlo simulation, while $\epsilon_{b\bar{b}}$ is measured from an unbiased $Z \rightarrow b\bar{b}$ data sample [6] and corrected to take into account the presence of an energetic D meson in the opposite hemisphere. The systematic error on f_c arises mainly from the uncertainty on this correction [5]. The measured charm fractions are listed in Table 2.

The b asymmetry A_{FB}^b is fixed to the Standard Model values at the three centre of mass energies, as listed in Table 3, together with the dependence of the fitted charm asymmetry. The effective asymmetry that enters in this analysis is diluted by a factor $(1 - 2\chi_{\text{mix}})$, due to the mixing of neutral b mesons. The mixing probability χ_{mix} is different for each reconstructed D meson, since it depends on the fraction of such mesons produced in B^0 decays among all $b \rightarrow D^{*\pm}, D^0, D^+$ decays. These fractions are derived from Monte Carlo simulations and the associated errors are taken as the difference between the Monte Carlo prediction and an estimate based on experimental measurements in the semileptonic sector [7]. These values, together with the world average value of χ_d , are used to obtain the χ_{mix} values, shown in Table 2. The contribution from the double-charm decays of b hadrons, in which the charge of

Table 2: Charm fraction and mixing probability used to extract the charm asymmetry from the observed asymmetry. The first column shows the charm fractions, as measured from data, with the statistical and systematic uncertainties. The second column shows the obtained fractions of $D^{*\pm}$'s, D^0 's and D^+ 's coming from B^0 decays among all $b \rightarrow D^{*\pm}, D^0, D^+$ decays. The resulting values of χ_{mix} are listed in the last column.

Decay channel	f_c	$\frac{B^0 \rightarrow D}{b \rightarrow D}$	χ_{mix}
$D^{*+} \rightarrow \pi_s^+ K^- \pi^+$	$0.741 \pm 0.019 \pm 0.007$	0.80 ± 0.05	0.16 ± 0.04
$D^{*+} \rightarrow \pi_s^+ K^- \pi^+ \pi^0$	$0.743 \pm 0.019 \pm 0.007$	0.80 ± 0.05	0.16 ± 0.04
$D^0 \rightarrow K^- \pi^+$	$0.787 \pm 0.019 \pm 0.006$	0.22 ± 0.05	0.035 ± 0.005
$D^{*+} \rightarrow \pi_s^+ K^- \pi^+ \pi^+ \pi^-$	$0.783 \pm 0.016 \pm 0.006$	0.80 ± 0.05	0.16 ± 0.04
$D^{*+} \rightarrow \pi_s^+ K^- \pi^+ (\pi^0)$	$0.766 \pm 0.021 \pm 0.007$	0.80 ± 0.05	0.16 ± 0.04
$D^+ \rightarrow K^- \pi^+ \pi^+$	$0.797 \pm 0.020 \pm 0.006$	0.72 ± 0.03	0.12 ± 0.02

Table 3: Value of A_{FB}^b at the three energy points, used to extract A_{FB}^c . These value correspond to the Standard Model prediction with $m_t = 175 \text{ GeV}/c^2$, $m_H = 127 \text{ GeV}/c^2$ and $\alpha_s = 0.120$, without QCD correction in the final state (a discussion of the corrections to the asymmetry in this analysis follows in the text). The last column shows the dependence of the charm asymmetry on the value of A_{FB}^b .

$\sqrt{s}(\text{GeV})$	$A_{FB}^b(\%)$	dA_{FB}^c/dA_{FB}^b
89.37	5.7	-0.22
91.22	9.7	-0.22
92.96	12.1	-0.22

the reconstructed $D^{(*)}$ has the opposite sign with respect to single-charm decays, is negligible due to the low momentum of the decay products [8].

The doubly Cabibbo suppressed decay $D^0 \rightarrow K^+ \pi^-$, which affects both the charm and the b component of the inclusive D^0 sample, has a negligible effect on the results. The asymmetries are corrected to take into account the fraction of the selected $D^{(*)}$'s that originate from gluon splitting, estimated to be $(0.8 \pm 0.4)\%$ [5].

The asymmetry of the combinatorial background is measured from the upper side band of the mass peaks. Within the side bands, multiply-counted events are selected only once by choosing the candidate randomly. In the case of the D^+ , the contributions of the resonant backgrounds are negligible in the upper side band region. On the other hand, in the case of the $D^0 \rightarrow K^- \pi^+$ channel, the side band sample contains a contribution where the two mass assignments of the D^0 decay products are reversed. This contribution induces an asymmetry opposite to the real asymmetry. Its size (around 5% of the side band sample) is estimated from the Monte Carlo simulation and then subtracted from the measured background asymmetry, using the Standard Model values for the charm and b asymmetries. The correction shifts the measured D^0 background asymmetry by 0.004. The combinatorial background asymmetries for all channels, measured at the three centre of mass energies, are listed in Table 4.

The charm asymmetry is extracted by means of an unbinned maximum likelihood

Table 4: *Combinatorial background asymmetries, measured on data, at the three centre of mass energies, from the side band of the mass peaks.*

Decay channel	peak - 2 GeV	peak	peak + 2 GeV
$D^{*+} \rightarrow \pi_s^+ K^- \pi^+$	0.001 ± 0.045	0.0050 ± 0.0092	-0.013 ± 0.036
$D^{*+} \rightarrow \pi_s^+ K^- \pi^+ \pi^0$	0.016 ± 0.024	0.0063 ± 0.0050	0.045 ± 0.019
$D^0 \rightarrow K^- \pi^+$	-0.105 ± 0.060	-0.005 ± 0.013	-0.015 ± 0.048
$D^{*+} \rightarrow \pi_s^+ K^- \pi^+ \pi^+ \pi^-$	0.021 ± 0.014	0.0035 ± 0.0029	0.011 ± 0.011
$D^{*+} \rightarrow \pi_s^+ K^- \pi^+ (\pi^0)$	0.036 ± 0.028	-0.0026 ± 0.0057	0.006 ± 0.021
$D^+ \rightarrow K^- \pi^+ \pi^+$	0.016 ± 0.024	0.0015 ± 0.0052	-0.004 ± 0.020

Table 5: *Sources of systematic errors on the measured charm forward-backward asymmetry. The total errors are obtained summing in quadrature the relative contributions.*

Source	ΔA_{FB}^c (%)		
	peak - 2 GeV	peak	peak + 2 GeV
Fraction of D mesons f_{sig}	± 0.15	± 0.10	± 0.22
Charm fraction f_c	± 0.10	± 0.02	± 0.12
b mixing	± 0.09	± 0.17	± 0.18
Comb. back. asymmetry	± 0.98	± 0.20	± 0.75
Gluc. splitting	—	± 0.03	± 0.05
TOTAL	± 1.00	± 0.28	± 0.81

fit giving the following results at the three different centre of mass energies:

$$\begin{aligned}
 A_{FB}^c(\sqrt{s} = 89.37 \text{ GeV}) &= (-1.0 \pm 4.3 \pm 1.0)\% \\
 A_{FB}^c(\sqrt{s} = 91.22 \text{ GeV}) &= (6.3 \pm 0.9 \pm 0.3)\% \\
 A_{FB}^c(\sqrt{s} = 92.96 \text{ GeV}) &= (11.0 \pm 3.3 \pm 0.8)\% .
 \end{aligned}$$

The first error is statistical and the second arises from systematic uncertainties as listed in Table 5. The angular distribution of the tagged $Z \rightarrow c\bar{c}$ events at the Z is shown in Figure 4, after background subtraction and acceptance corrections. Figure 5 shows the measured asymmetries as a function of the centre of mass energy together with the predictions of the Standard Model.

The pole asymmetry as defined in Eq. 2 is extracted from the measured asymmetries at the three energy points by expressing them as a single measurement at the Z mass and applying a correction for the effect of initial and final state radiation, QCD corrections and photon exchange and interference. As pointed out in Ref. [9], the theoretical estimate of the QCD correction has to be rescaled to take into account the bias from the experimental cuts. In particular, the requirement of high momentum $D^{(*)}$ s removes events in which hard gluon emission occurred, substantially reducing the correction. As computed from Monte Carlo, the relative QCD correction after selection cuts are found to be consistent with zero within a 0.14% absolute uncertainty. The initial state radiation correction can also be biased by the selection cuts, which are less efficient at lower centre of mass energies. This correction, calculated to be 14.9% using the MIZA program [10], is lowered to $(14.1 \pm 0.1)\%$ when the selection bias is taken

into account. The final relative correction to be applied to the measured asymmetry at the energy of the Z mass is $(13.2 \pm 0.2)\%$.

Within the Standard Model, the measured asymmetry can be used to extract a value of $\sin^2 \theta_W^{\text{eff}}$, taking into account the dependence of the b asymmetry on this quantity, yielding

$$\sin^2 \theta_W^{\text{eff}} = 0.2321 \pm 0.0016 .$$

5 Conclusion

The forward-backward asymmetry in $Z \rightarrow c\bar{c}$ decays has been measured at three different energies, at the Z peak and off-peak at ± 2 GeV:

$$\begin{aligned} A_{FB}^c(\sqrt{s} = 89.37 \text{ GeV}) &= (-1.0 \pm 4.4)\% \\ A_{FB}^c(\sqrt{s} = 91.22 \text{ GeV}) &= (6.3 \pm 1.0)\% \\ A_{FB}^c(\sqrt{s} = 92.96 \text{ GeV}) &= (11.0 \pm 3.4)\% . \end{aligned}$$

A Standard Model fit to the measured asymmetries yields $\sin^2 \theta_W^{\text{eff}} = 0.2321 \pm 0.0016$. These measurements are in agreement with the Standard Model predictions and with the other determinations of these parameters at LEP [11].

Acknowledgements

We thank our colleagues from the accelerator divisions for the successful operation of the LEP machine and the engineers and technical staff in all our institutions for their contribution to the good performance of ALEPH. Those of us from non-member states thank CERN for its hospitality.

References

- [1] ALEPH Collaboration, *ALEPH: A Detector for Electron - Positron Annihilations at LEP*, Nucl. Instr. Methods **A294** (1990) 121.
- [2] ALEPH Collaboration, *Performance of the ALEPH detector at LEP*, Nucl. Instr. Methods **A360** (1995) 481.
- [3] ALEPH Collaboration, *Production of charmed mesons in Z decays*, Z. Phys. **C62** (1994) 1.
- [4] R.M. Barnett *et al.* (Particle Data Group), Phys. Rev. **D54** (1996) 1.
- [5] ALEPH Collaboration, *Measurement of the fraction of hadronic Z decays into charm quark pairs*, CERN-EP/98-035, to be published in Eur. Phys. J. C
- [6] ALEPH Collaboration, *A Measurement of R_b using a lifetime mass tag*, Phys. Lett. **B401** (1997) 150; *A Measurement of R_b using mutually exclusive tags*, Phys. Lett. **B401** (1997) 163.
- [7] ALEPH Collaboration, *Improved Measurement of the \bar{B}^0 and B^- meson Lifetimes*, Z. Phys. **C71** (1996) 31.

- [8] ALEPH Collaboration, *Observation of doubly-charmed B decays at LEP*, CERN-EP/98-037, submitted to Eur. Phys. J. C.
- [9] D. Abbaneo *et al.*(LEP Heavy Flavour Working Group), CERN-EP/98-032, submitted to Eur. Phys. J. C.
- [10] M. Martinez *et al.*, Z. Phys. **C49** (1991) 645.
- [11] The LEP Collaborations ALEPH, DELPHI, L3, OPAL, the LEP Electroweak Working Group and the SLD Heavy Flavour Group, *A Combination of Preliminary Electroweak Measurements and Constraints on the Standard Model*, CERN-PPE/97-154.

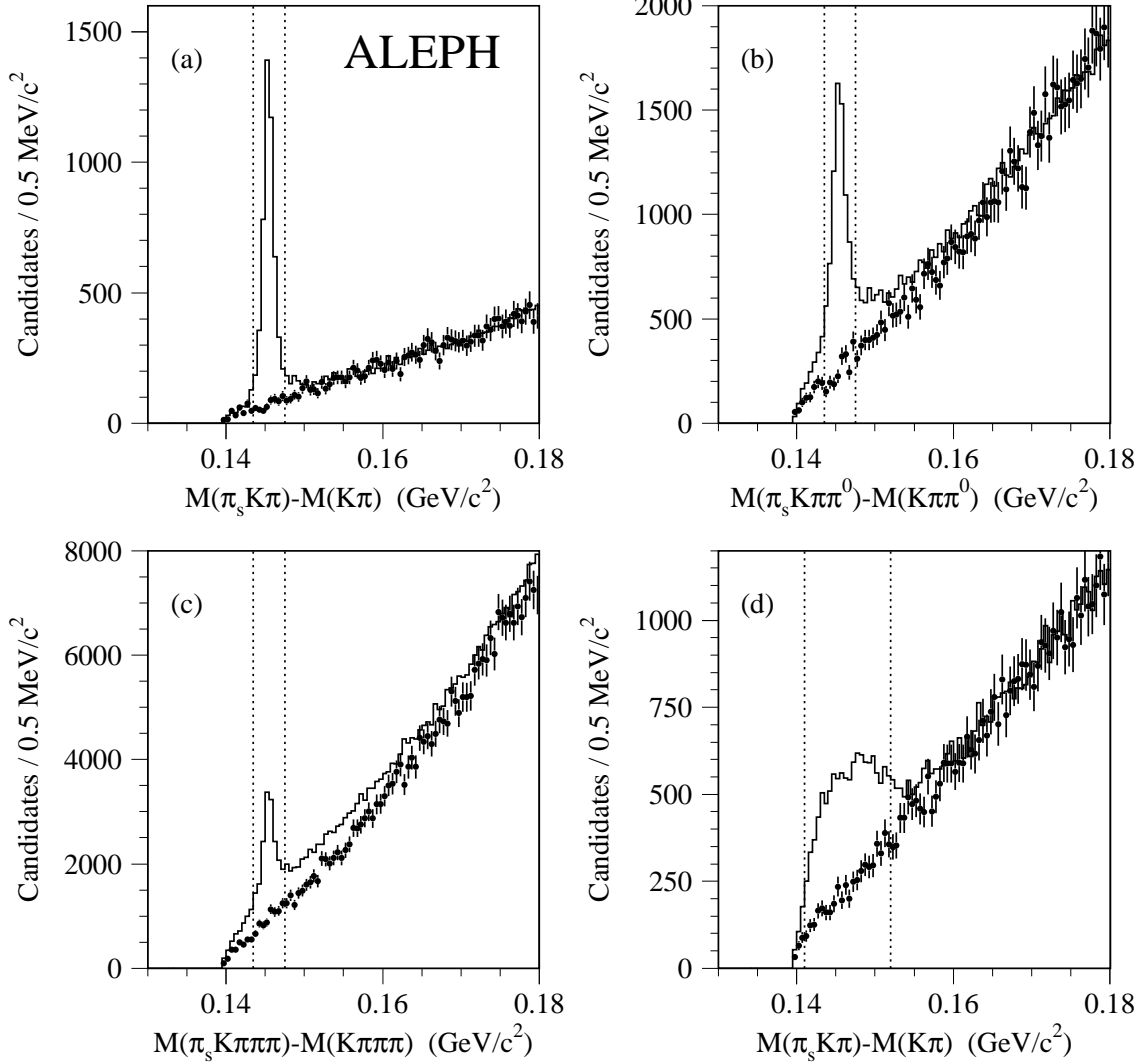


Figure 1: *Mass-difference distribution for candidates of the decay channel $D^{*+} \rightarrow \pi_s^+ D^0$, followed by $D^0 \rightarrow K^- \pi^+$ (a), $D^0 \rightarrow K^- \pi^+ \pi^0$ (b), $D^0 \rightarrow K^- \pi^+ \pi^+ \pi^-$ (c) and $D^0 \rightarrow K^- \pi^+ (\pi^0)$ (d). The full histogram are the data while the dots with error bars are the combinatorial background taken from Monte Carlo simulation. The error bars represent both the statistical error due to the limited Monte Carlo statistics and the systematic error in the normalisation. The dotted lines show the selected region.*

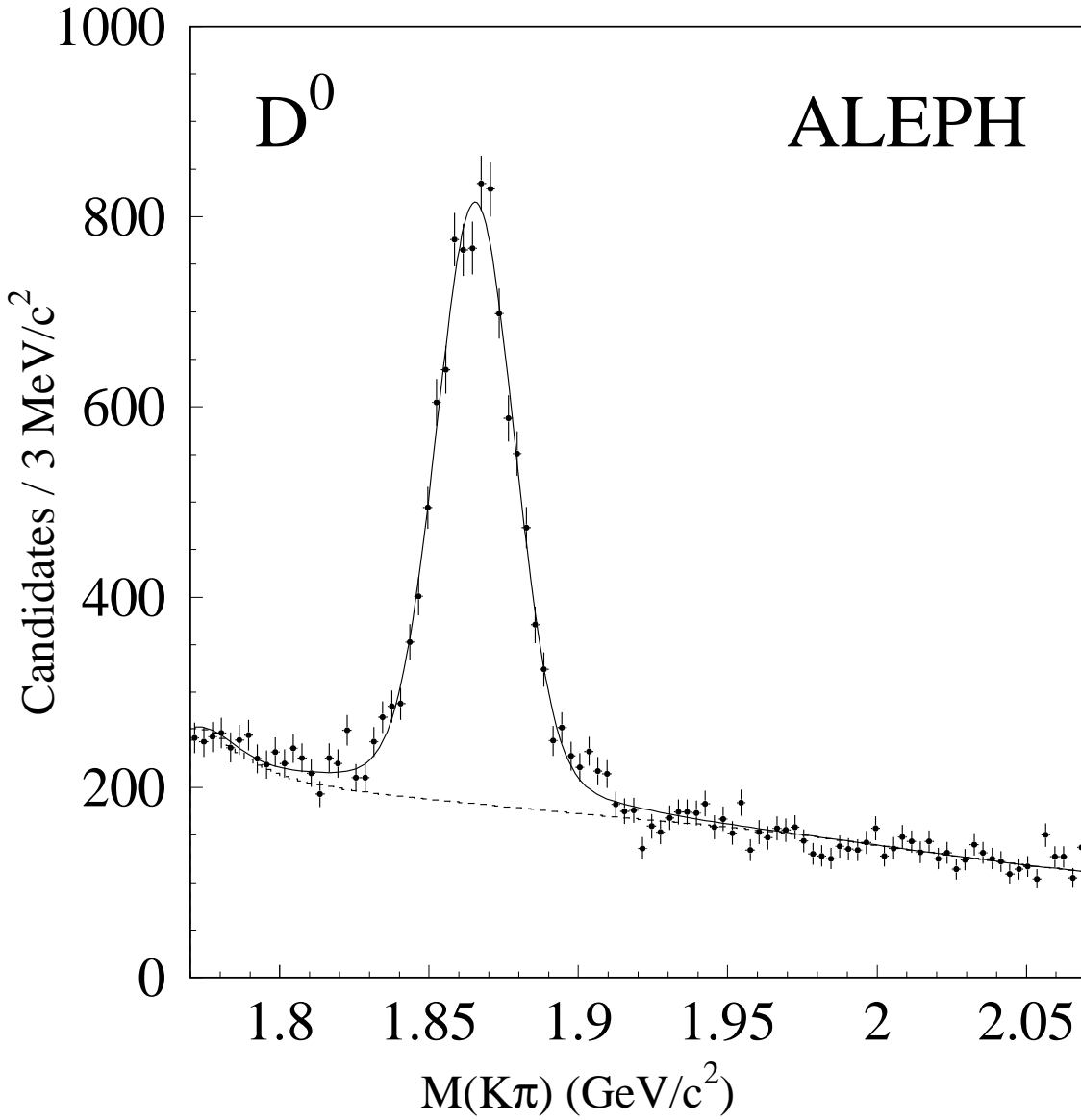


Figure 2: Mass distribution for candidates of the decay channel $D^0 \rightarrow K^- \pi^+$. The dots with error bars are data while the solid line represent the best fit to the distribution and the dashed line is the best fit to the background.

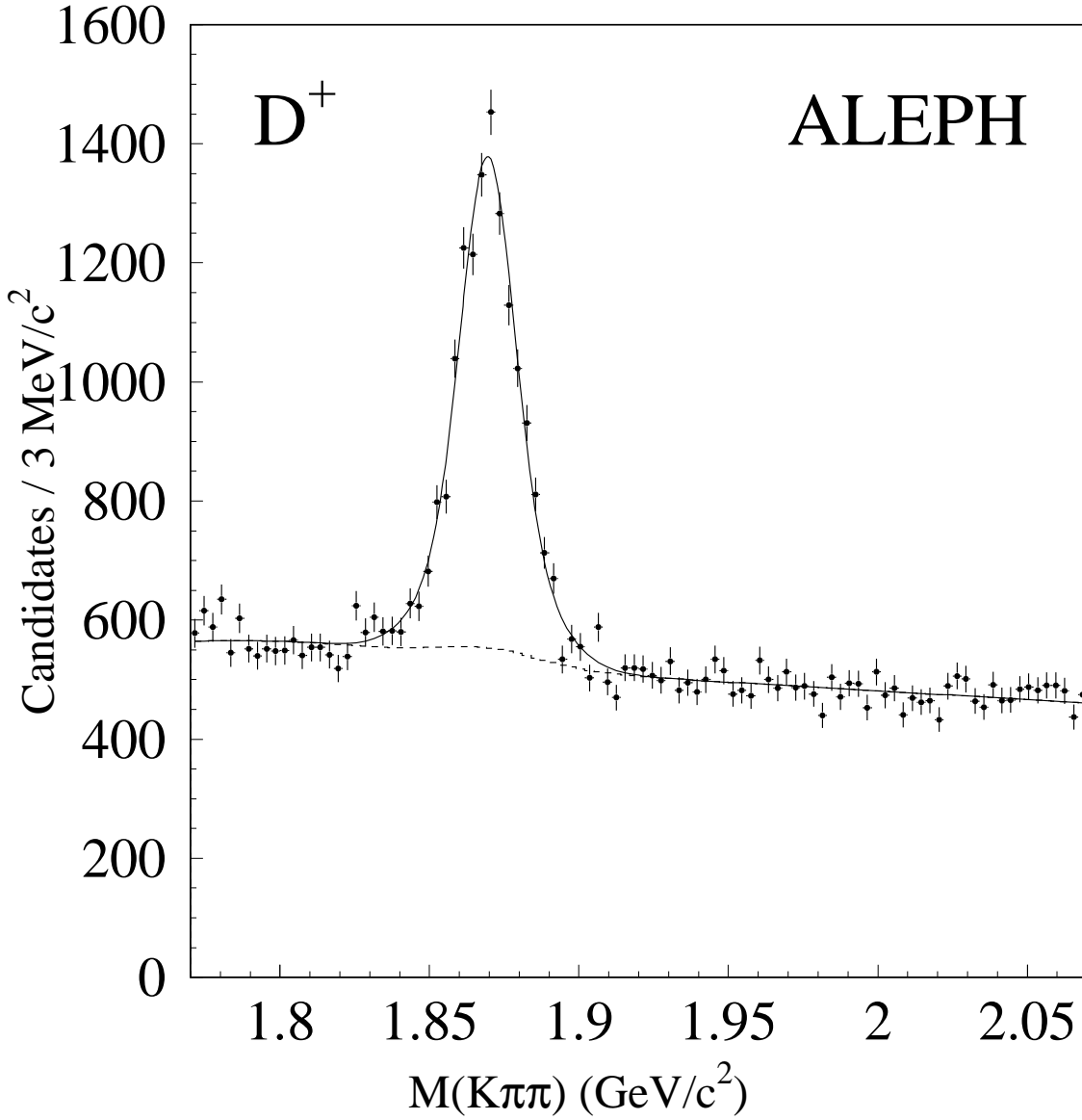


Figure 3: Mass distribution for candidates of the decay channel $D^+ \rightarrow K^- \pi^+ \pi^+$. The dots with error bars are data while the solid line represent the best fit to the distribution and the dashed line is the best fit to the background.

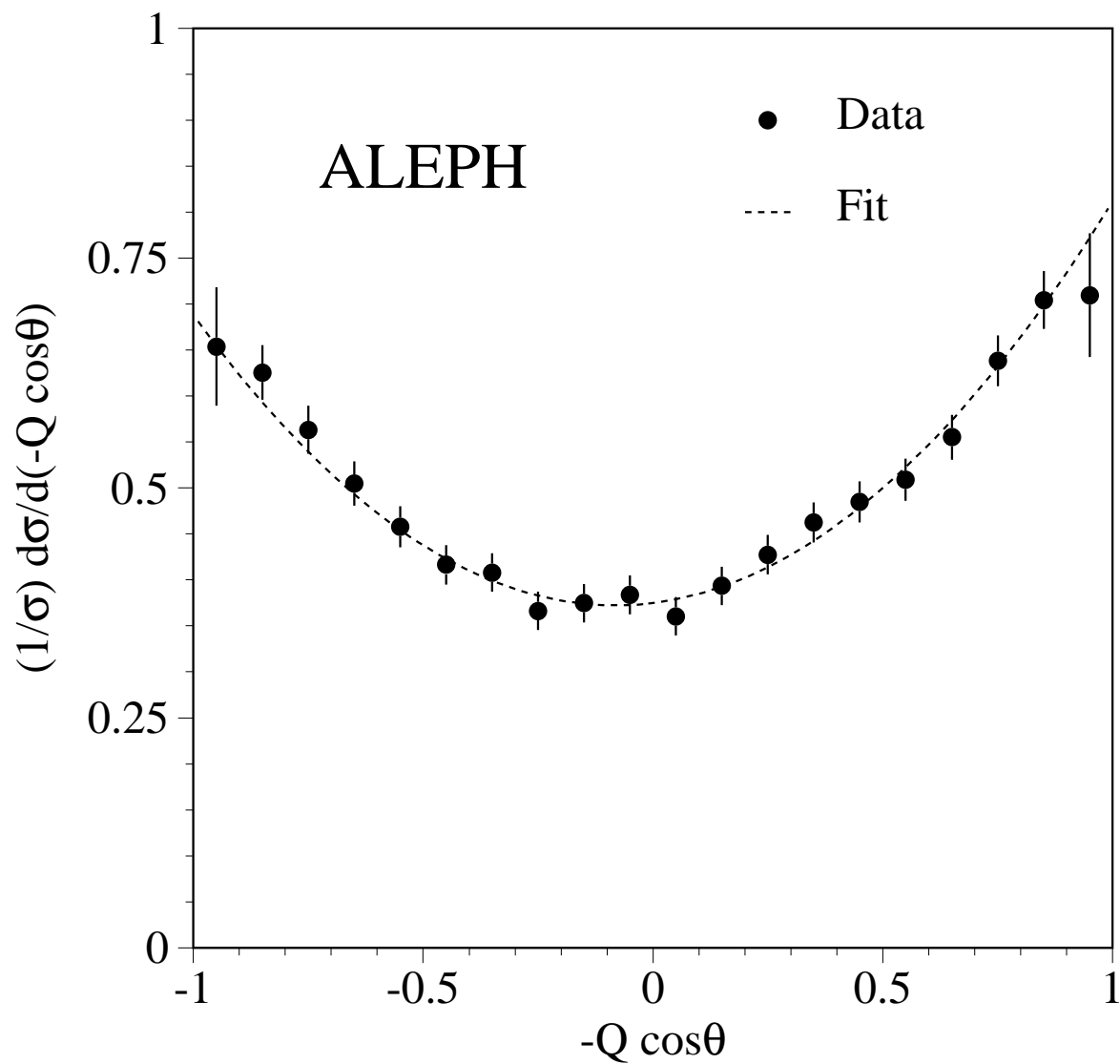


Figure 4: Normalized angular distribution of the tagged $Z \rightarrow c\bar{c}$ events at $\sqrt{s} = 91.2$ GeV, corrected for acceptance and background subtracted. The dots with error bars are data while the dashed line is the result of the fit.

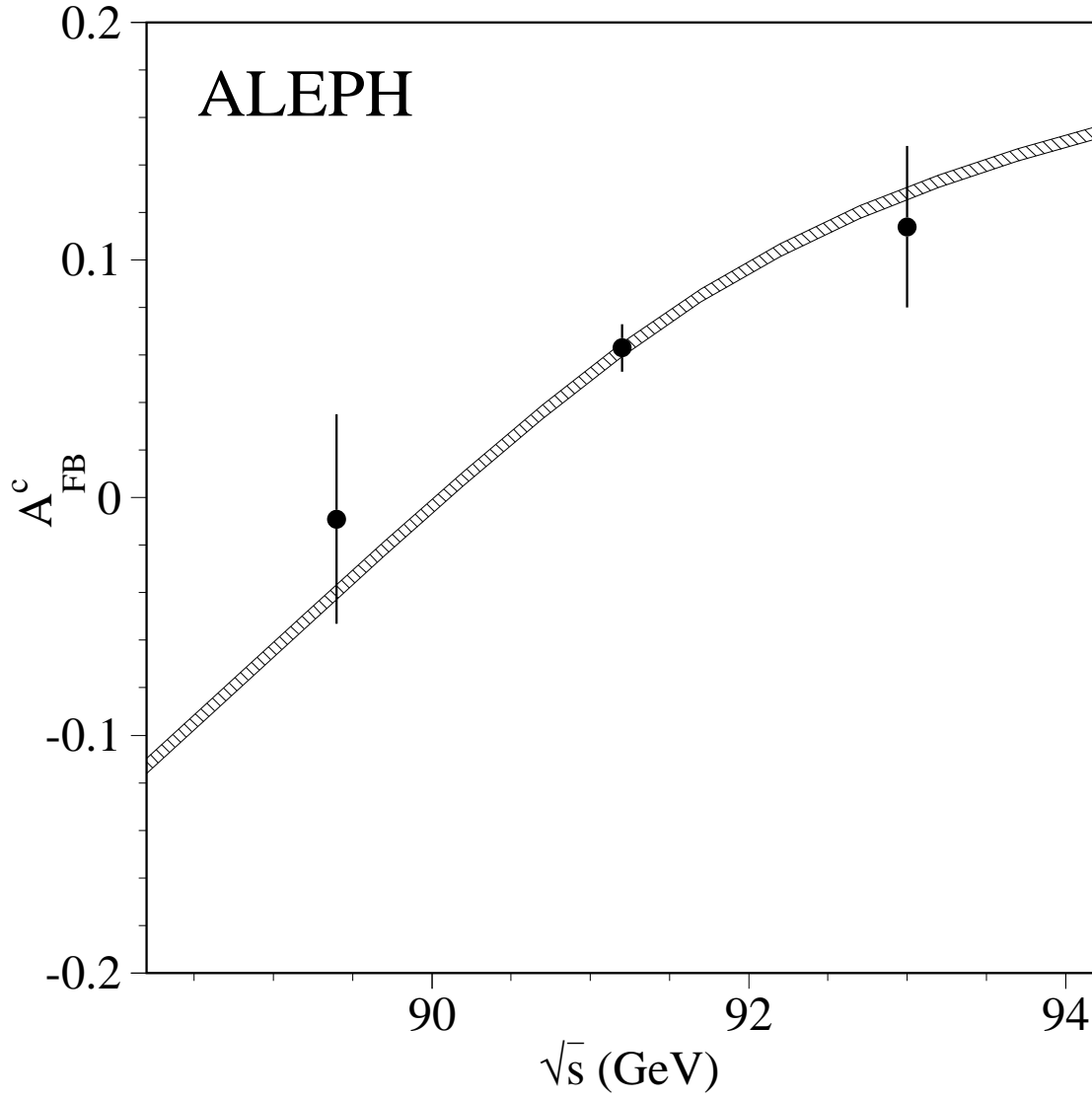


Figure 5: A_{FB}^c as a function of the centre of mass energy. The dots with error bars are the measured asymmetries. The curve is the prediction of the Standard Model with $m_t = 175 \text{ GeV}/c^2$, $m_H = [90, 1000] \text{ GeV}/c^2$ and $\alpha_s = 0.120$.